

# Changes in the Spectral Characteristics of Ventricular Fibrillation in Lesions Produced by Radiofrequency Ablation. An Experimental Study

Francisco J. Chorro,<sup>a,b</sup> Juan Guerrero,<sup>c</sup> Joaquín Cánoves,<sup>b</sup> Isabel Trapero,<sup>d</sup> Luis Mainar,<sup>b</sup> Francisca Pelechano,<sup>a</sup> Estrella Blasco,<sup>b</sup> Luis Such-Miquel,<sup>e</sup> Ángel Ferrero,<sup>b</sup> Juan Sanchis,<sup>a,b</sup> Vicente Bodí,<sup>a,b</sup> José M. Cerdá,<sup>f</sup> Antonio Alberola,<sup>g</sup> and Luis Such<sup>g</sup>

<sup>a</sup>Departamento de Medicina, Universidad de Valencia (UVEG), Valencia, Spain

<sup>b</sup>Servicio de Cardiología, Hospital Clínico Universitario, Valencia, Spain

<sup>c</sup>Departamento de Electrónica, Universidad de Valencia (UVEG), Valencia, Spain

<sup>d</sup>Departamento de Enfermería, Universidad de Valencia (UVEG), Valencia, Spain

<sup>e</sup>Departamento de Fisioterapia, Universidad de Valencia (UVEG), Valencia, Spain

<sup>f</sup>Departamento de Anatomía Patológica, Universidad de Valencia (UVEG), Valencia, Spain

<sup>g</sup>Departamento de Fisiología, Universidad de Valencia (UVEG), Valencia, Spain

**Introduction and objectives.** Although electrophysiological databases contain information about changes in the time domain in lesions produced by radiofrequency ablation, very few data on changes in the frequency domain are available. The aim of this study was to investigate changes in the spectral characteristics of ventricular fibrillation in zones with radiofrequency lesions.

**Methods.** Recordings of ventricular fibrillation were obtained in 11 isolated perfused rabbit heart preparations using a multiple epicardial electrode located on the left ventricular free wall. Spectral parameters derived by Fourier analysis before and after the creation of transmural radiofrequency lesions were compared.

**Results.** In the ablated zones, significant reductions were observed in the spectral density of the dominant ( $0.168 [0.113] \text{ mV}^2/\text{Hz}$  vs  $0.025 [0.018] \text{ mV}^2/\text{Hz}$ ;  $P < .001$ ) and mean frequencies ( $0.053 \pm 0.057 \text{ mV}^2/\text{Hz}$  vs  $0.012 [0.016] \text{ mV}^2/\text{Hz}$ ;  $P < .001$ ), the normalized energy around the dominant frequency ( $0.860 [0.570]$  vs  $0.128 [0.091]$ ;  $P < .001$ ), and the standard deviation of the power spectrum ( $0.031 [0.020] \text{ mV}^2/\text{Hz}$  vs  $0.004 [0.001] \text{ mV}^2/\text{Hz}$ ;  $P < .001$ ). There was no significant change in the dominant ( $16.2 [5.6]$  vs  $14.8 [1.8] \text{ Hz}$ ) or mean frequency ( $17.7 [3.4]$  vs  $16.6 [1.3] \text{ Hz}$ ). The spectral parameters that could be used in a multivariate model to identify the lesion were the standard deviation of the power spectrum and the spectral density of the mean frequency.

**Conclusions.** During ventricular fibrillation, the spectral parameters associated with spectral power and spectral

energy were significantly altered in zones with radiofrequency lesions and could be used to identify those zones. There was no significant change in either the dominant or mean frequency in these zones.

**Key words:** Ventricular fibrillation. Radiofrequency ablation. Fourier analysis.

## Modificaciones de las características espectrales de la fibrilación ventricular en las lesiones producidas con radiofrecuencia. Estudio experimental

**Introducción y objetivos.** Aunque se dispone de información sobre las modificaciones en el dominio del tiempo de los registros electrofisiológicos en zonas lesionadas con radiofrecuencia, los datos disponibles en el dominio de la frecuencia son muy escasos. Se analizan las modificaciones de las características espectrales de la fibrilación ventricular en zonas lesionadas con radiofrecuencia.

**Métodos.** En 11 preparaciones de corazón aislado y perfundido de conejo, se registra la fibrilación ventricular con un electrodo múltiple epicárdico situado en la pared libre ventricular izquierda. Se comparan los parámetros espectrales obtenidos mediante análisis de Fourier antes y después de practicar lesiones transmurales con radiofrecuencia.

**Resultados.** En las zonas lesionadas disminuye significativamente la densidad espectral de las frecuencias dominante ( $0,168 \pm 0,113$  y  $0,025 \pm 0,018 \text{ mV}^2/\text{Hz}$ ;  $p < 0,001$ ) y media ( $0,053 \pm 0,057$  y  $0,012 \pm 0,016 \text{ mV}^2/\text{Hz}$ ;  $p < 0,001$ ), la energía normalizada alrededor de la frecuencia dominante ( $0,860 \pm 0,570$  y  $0,128 \pm 0,091$ ;  $p < 0,001$ ) y la desviación típica del espectro de potencias ( $0,031 \pm 0,020$  y  $0,004 \pm 0,001 \text{ mV}^2/\text{Hz}$ ;  $p < 0,001$ ). No se modifican significativamente las frecuencias dominante ( $16,2 \pm 5,6$  y  $14,8 \pm 1,8 \text{ Hz}$ ) y media ( $17,7 \pm 3,4$  y  $16,6 \pm 1,3 \text{ Hz}$ ). Los parámetros espectrales aceptados en el modelo multivariable para indicar que los registros se efectúan en la lesión

Funding for this study was provided by Instituto de Salud Carlos III, Ministerio de Sanidad y Consumo, PI06/0758, RETIC RD06/0003/0010 (REDINSCOR), and Sociedad Española de Cardiología (grant number 2005).

Correspondence: Dr. F. J. Chorro.  
Servicio de Cardiología. Hospital Clínico Universitario.  
Avda. Blasco Ibáñez, 17. 46010 Valencia. España.  
E-mail: Francisco.J.Chorro@uv.es

Received August 27, 2007.

Accepted for publication January 8, 2008.

son la desviación típica del espectro de potencias y la densidad espectral de la frecuencia media.

**Conclusiones.** Durante la fibrilación ventricular, los parámetros relacionados con la potencia y la energía espectral muestran modificaciones significativas en las zonas lesionadas con radiofrecuencia y pueden ayudar a identificarlas. Las frecuencias dominante y media no se modifican significativamente en las zonas lesionadas.

**Palabras clave:** Fibrilación ventricular. Ablación con radiofrecuencia. Análisis de Fourier.

#### ABBREVIATIONS

DFr: dominant frequency  
En: frequency spectrum energy  
MFr: mean frequency  
RF: radio-frequency  
RMS: root mean square  
VF: ventricular fibrillation

## INTRODUCTION

Analysis of the characteristics of electrophysiological signals can help to identify regions of interest associated with the mechanisms involved in different types of arrhythmias. The information obtained can facilitate selective interventions involving radiofrequency ablation (RF).<sup>1,2</sup> In this sense, locating areas of post-infarct scarring has proved to be useful in identifying target zones during treatment of ventricular tachycardia.<sup>3-6</sup>

On the other hand, RF also modifies the substrate and thereby alters the characteristics of the signals recorded. Although information is available on changes in the time domain of atrial and ventricular signals in regions with RF lesions,<sup>7-13</sup> information on changes in the frequency domain is scarce. This should be taken into account when interpreting recordings obtained during RF ablation procedures or in patients who have undergone ablation procedures.

Spectral techniques are used to analyze both atrial and ventricular (VF) fibrillation. The information provided includes the frequency domain of the spectrum, which is directly related to myocardial activation frequency.<sup>14-19</sup> Using these techniques it is possible to identify regions<sup>20,21</sup> which may be of interest for local interventions. Spectral analysis can likewise help to detect fibrillatory

processes, define their characteristics, and apply automatic defibrillation procedures.

RF ablation reduces electrogram amplitude in zones with lesions, but information is not available about its effects on spectral characteristics, including parameters such as signal frequency which are related with spectral power and energy. In the present study, an experimental model with isolated rabbit heart preparations was used to evaluate the hypothesis that the spectral characteristics of VF recordings obtained in zones with RF lesions would be significantly altered and that these alterations, as well as those observed in the time domain, could be helpful in determining whether recordings were performed in zones with lesions.

## METHODS

### Experimental Preparation

The procedures used in this study followed current guidelines on the care and use of animals in research laboratories. Isolated perfused New Zealand rabbit hearts (n=11; weight, 2.7 [0.3] kg) were used. After anesthesia (ketamine 25 mg/kg im) and heparinization, the heart was removed and submerged in cold Tyrode's solution (4°C). After isolating the aorta, a Langendorff system was connected to perfuse Tyrode, as in earlier studies.<sup>18,19</sup> Ventricular electrograms were recorded using a multiple electrode, composed of 235 unipolar electrodes (diameter, 0.125 mm; distance between electrodes, 1 mm; surface covered, 225 mm<sup>2</sup>), located on the epicardium of the left ventricular free wall. An Ag-AgCl reference electrode located above the aorta was used. Ventricular stimulation was performed using a bipolar electrode and a GRASS S88 stimulator with a stimulus isolation unit (SIU5). The recordings were obtained using a cardiac mapping system (MAPTECH) with frequency bands between 1 and 400 Hz. VF was induced using increasing frequency stimulation. Perfusion was maintained during the arrhythmia. Recordings were obtained at baseline and after performing a transmural RF lesion in the left ventricular wall from the base to the middle zone of free wall (Figure 1). A needle electrode was used to produce the lesion (diameter, 0.5 mm) through top down consecutive punctures in the ventricular wall. At each puncture site, RF was applied at 10 W for 20 s, using an Osypka HAT 100 generator. The dispersive pad was located on the aortic cannula used for perfusion. After administering RF, VF recordings were obtained after an interval of at least 10 min, with the multiple electrode located at the same position and covering both the zone with the lesion and the surrounding undamaged myocardium. Four fixed points marked on the ventricular wall were used to ensure that the electrode was always located in the same position.

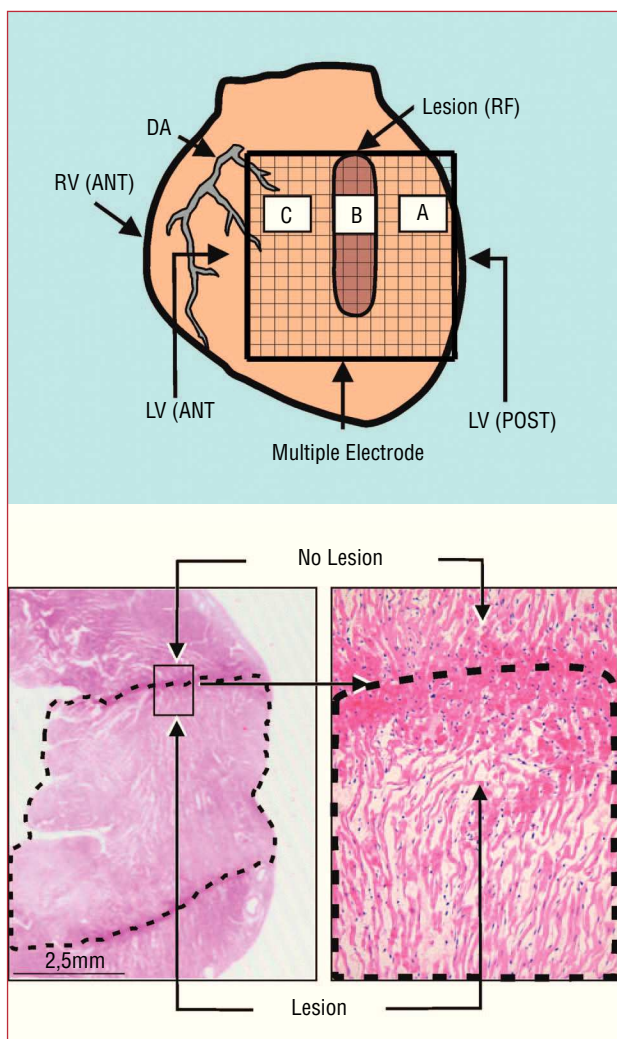


**Figure 1.** Upper: diagram showing the multiple electrode on the zones with (B) and without (A and C) lesions. Lower: section of the left ventricular wall with the lesion (dotted line) produced by radio-frequency (HE,  $\times 4$ ). The lesion is trans-mural and well-defined. On the right, one of the edges of the damaged zone is shown (HE,  $\times 25$ ). DA indicates descending anterior artery; LV(ANT), left anterior ventricle; LV(POST), left posterior ventricle; RV(ANT), right anterior ventricle.

## Data Analyzed

### Electrogram Spectral Analysis During VF

Welch's method<sup>22</sup> was used to obtain the power spectrum (Figure 2) of the signals recorded with 15 unipolar electrodes located in the 3 selected zones (5 electrodes for each) (Figure 1). Zone A corresponded to undamaged tissue and was located 4 mm to the right of the lesion, zone B was in the center of the lesion, and zone C corresponded to undamaged tissue 4 mm to the left of the lesion. We analyzed blocks of 4096 points (sampling frequency, 1 kHz) without zero padding. Data were processed with Matlab running on the Hewlett-

Packard 712/80 platform. The following parameters were determined:

- DFr: dominant frequency (Hz) or frequency of the power spectrum with the greatest amplitude, determined at a resolution of 0.5 Hz
- MFr: mean spectral frequency (Hz)
- densDFr: spectral density of the dominant frequency ( $\text{mV}^2/\text{Hz}$ )
- densMFr: spectral density of the mean frequency ( $\text{mV}^2/\text{Hz}$ )
- EnDFr: normalized spectral energy around the dominant frequency (DFr [1] Hz) (dimensionless)
- SDPSp: standard deviation of the power spectrum ( $\text{mV}^2/\text{Hz}$ )

### Electrogram Time-Domain Analysis During VF

The following morphological characteristics of the electrograms were determined within the same time window:

- MAmpl: mean signal amplitude (mV)
- SDAmpl: standard deviation of the signal amplitude (mV)
- RMSAmpl: root mean square of the signal amplitude (mV)
- MdV/dt: mean dV/dt of the maximum negative slope of the electrograms (mV/ms)
- SDDV/dt: standard deviation of the maximum negative slope of the electrograms (mV/ms)

## Statistical Analysis

Numerical data were expressed as mean (1 standard deviation [SD]). Comparison tests were carried out using a repeated measures generalized linear model in which study phase and zones were included as factors. The Bonferroni test was applied in the post-hoc analysis. Differences were considered statistically significant at  $P < .05$ . ROC (receiver operating characteristic) curves were calculated (sensitivity with respect to 1-specificity) for each parameter. To identify the parameters which most accurately identified recordings made in a damaged zone, stepwise logistic regression was performed; the state variable was whether or not the recording was made in the zone with the lesion. Variables included in the model were those which independently contributed to identifying the state variable. Analyses were performed using the SPSS statistical package.

## RESULTS

The RF lesions had a mean width and length of 3.2 (0.4) and 11.4 (0.6) mm, respectively. Macroscopic and microscopic analysis indicated that lesions were trans-mural and well-defined (Figure 1).

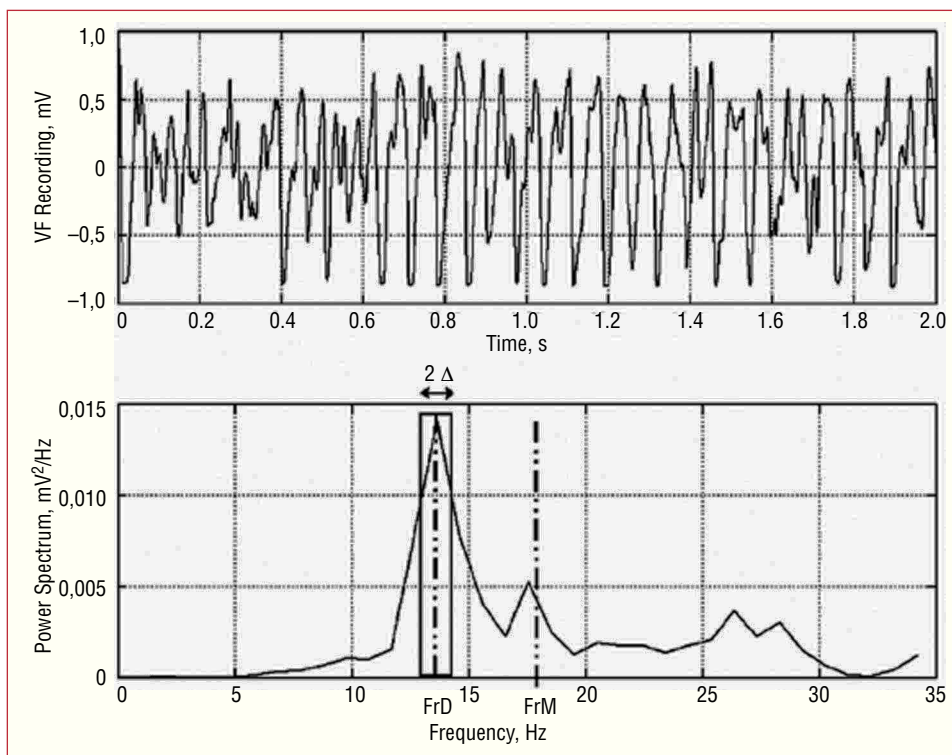


**Figure 2.** Power spectrum for one of the VF recordings. The dominant frequency (DFr) and its spectral density is shown, together with the mean frequency (MFr), and the spectral power in the DFr (1 Hz ( $2 \Delta$ )) band used to calculate the normalized energy around DFr. A total of 2 s of VF are shown to improve observation of the signal. The spectral analysis used 4 s segments.

### Frequency Domain Parameters

At baseline, before RF, there were no statistically significant differences between the 3 zones studied in terms of densDFr, densMFr, EnDFr, and SDPsp (Figure 3). DFr was significantly greater in zone C (zone A, 14.9 [5.2] Hz; zone B, 16.2 [5.6] Hz; zone C, 17.9 [4.2] Hz;  $P < .01$ ). There were no statistically significant differences in MFr values (zone A, 17.4 [3.2] Hz; zone B, 17.7 [3.4] Hz; zone C, 18.8 [3.2] Hz).

After the lesions were produced, densDFr, densMFr, EnDFr, and SDPsp decreased significantly in zone B (zone with lesion). Differences with the undamaged zones were also statistically significant (Figures 3 and 4). DFr and MFr did not vary significantly in zone B (DFr after RF, 14.8 [1.8] Hz, non-significant with respect to control; MFr after RF, 16.6 [1.3] Hz, non-significant with respect to control). In the zones without lesions, no significant before-after variations were observed, except for DFr in zone C, which decreased significantly (DFr after RF, 14.9 [2.8] Hz;  $P < .001$  compared to control).

### Time Domain Parameters

At baseline, differences were observed between zones B and C on the MAmpl, SDAmpl, MdV/dt and SDdV/dt variables, and between zones A and B on the MdV/dt and SDdV/dt variables (Figure 3). RMSAmpl was

significantly lower in zone C than in zone B (2.193 [0.707] and 2.520 [0.593];  $P < .05$ ). After RF, MAmpl, SDAmpl, SDdV/dt, and RMSAmpl decreased significantly in zone B, and corresponding MdV/dt values were significantly less negative (Figure 5). Differences with respect to the zones without lesions were also significant. In this phase, statistically significant differences were observed between the MdV/dt and SDdV/dt of zones A and C; the difference in SDdV/dt was also present at baseline.

### Frequency Domain Predictive Models

When we examined each of the variables one by one to determine whether the recordings corresponded to a zone with a lesion, the area under the ROC curve was  $>0.8$  for all of the parameters, except DFr (area=0.53) and MFr (area=0.56) (Table 1). Table 1 shows the cut-points and their corresponding sensitivity and specificity.

The logistic regression analysis showed that the frequency domain variables which contributed independently to identifying a zone with a lesion were SDPsp and densMFr. Their corresponding odds ratio (OR) and 95% confidence intervals (CI) are shown in Table 2. The ORs are  $<1$  and indicate that, when the parameters are within the values established using the cut-points from the ROC analysis, the probability that the recordings were made in the damaged zone is statistically significant.

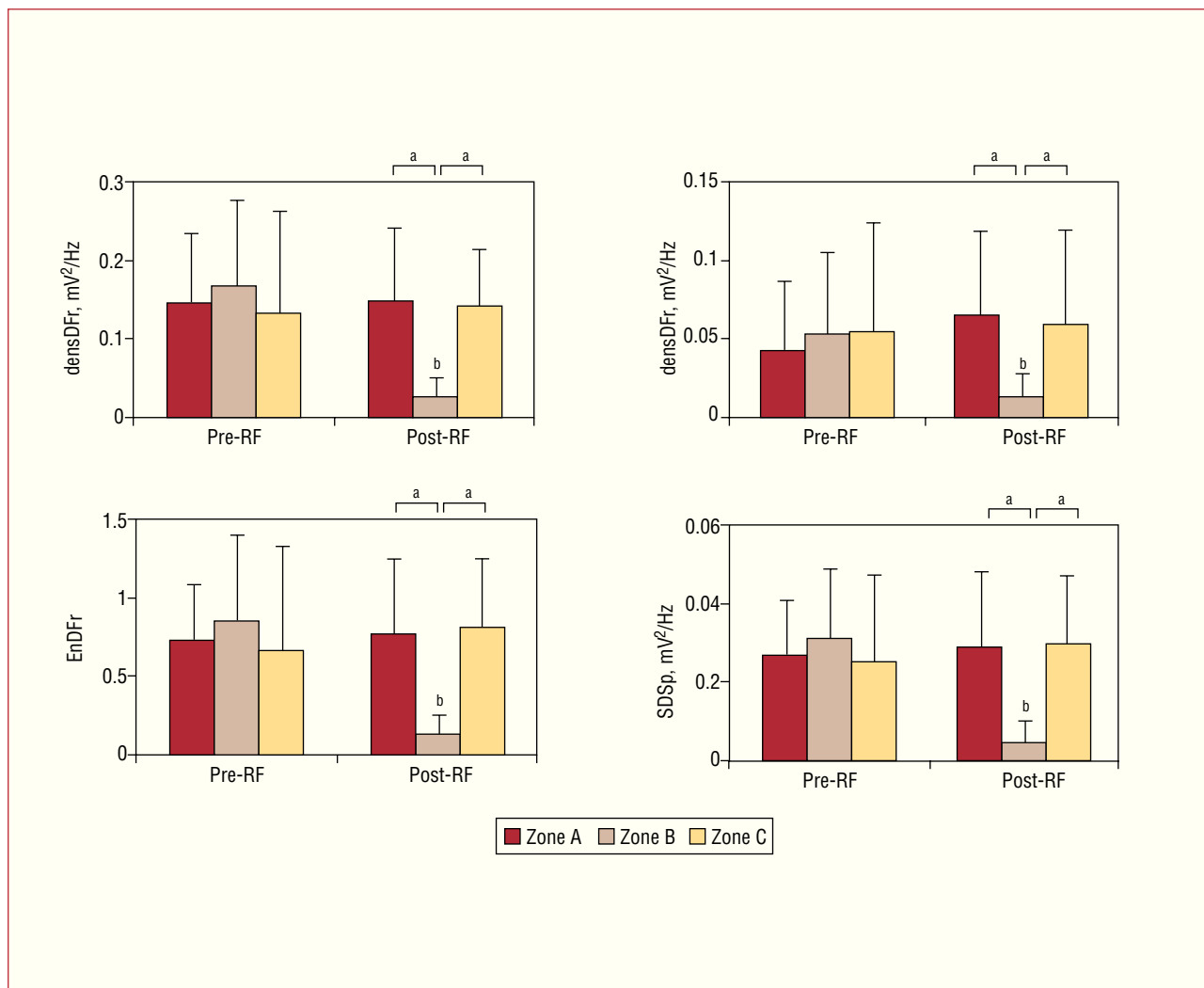


**Figure 3.** Values (mean [standard deviation]) of frequency domain parameters which varied significantly in the damaged zone. densDFr, spectral density of the dominant frequency; densMFr, spectral density of the mean frequency; EnDFr, normalized energy of the spectrum in the DFr (1) Hz band; RF, radio-frequency; zone B, zone with lesion; zones A and C, zones without lesions; SDSp indicates standard deviation of the power spectrum.

<sup>a</sup>Significant differences between zones: baseline and post-RF ablation.

<sup>b</sup>Significant differences with respect to baseline values.

### Time Domain Predictive Models

The area under the ROC curve for all variables was >0.9 in all cases. Table 1 shows the cut-points and their corresponding sensitivity and specificity. The logistic regression analysis showed that the time domain variables which contributed independently to identifying the zone with the lesion were MdV/dt and SDAmpl. Their corresponding odds ratio (OR) and 95% CI are shown in Table 2.

### DISCUSSION

The study's main findings are that: *a*) parameters associated with the spectral power and energy of VF

recordings were significantly altered in zones with radiofrequency lesions and that they could be used to identify zones with lesions; and *b*) there was no significant change in either the dominant or mean frequency in zones with lesions.

### Modification of VF Time Domain Characteristics in Zones With Lesions

RF thermal lesions cause coagulation necrosis which suppresses the myocardium's active electrical properties and alters the characteristics of the electrograms.<sup>23-29</sup> The structural damage makes it impossible to create action potentials and the tissue is converted into a passive or electrotonic transmission zone for potentials generated

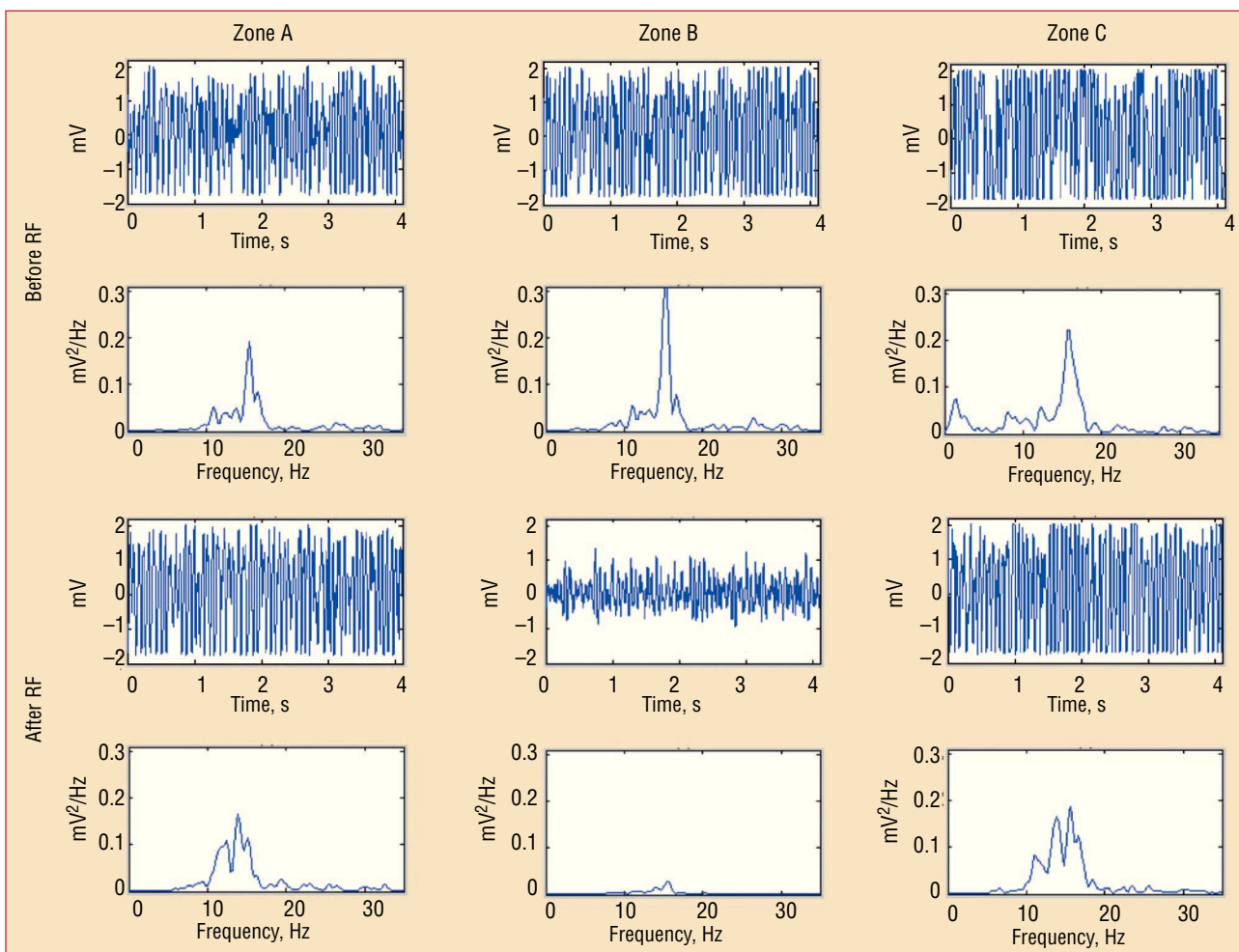


**Figure 4.** Electrograms of ventricular fibrillation and the corresponding power spectrum obtained from one of the electrodes located in each zone before and after radiofrequency. densDFr, spectral density of the dominant frequency; densMFr, spectral density of the mean frequency; EnDFr, normalized energy of the spectrum in the DFr (1) Hz band; RF, radio-frequency; SDPsp indicates standard deviation of the power spectrum; zone B, zone with lesion; zones A and C, zones without lesions.

**TABLE 1. Area Under the ROC Curve (Sensitivity vs 1–Specificity) and Cut-Point Values for the Best Univariate Parameters With Corresponding Sensitivity and Specificity Values**

	AUC	Cut-Point	Sensitivity	Specificity
Frequency domain				
densDFr, mV <sup>2</sup> /Hz	0.94	0.05	93%	84%
densMFr, mV <sup>2</sup> /Hz	0.83	0.011	80%	83%
EnDFr, normalized units	0.94	0.267	93%	86%
SDEsp, mV <sup>2</sup> /Hz	0.95	0.008	93%	87%
Time domain				
MAmpl, mV	0.98	0.247	98%	97%
SDAmp, mV	0.98	1.372	98%	93%
RMSAmp, mV	0.98	1.352	96%	94%
MdV/dt, mV/ms	0.99	-0.894	98%	99%
SDdV/dt, mV/ms	0.99	0.454	96%	95%

AUC indicates area under the ROC curve; densDFr, spectral density of the dominant frequency; densMFr, spectral density of the mean frequency; EnDFr, normalized energy of the spectrum in the DFr (1) Hz band; MAmp, mean amplitude of the signals recorded during ventricular fibrillation; MdV/dt, mean dV/dt; RMSAmp, root mean square of the VF signal amplitude; SDAmp, standard deviation of the signal amplitude in the ventricular fibrillation; SDdV/dt, standard deviation of dV/dt; SDEsp, standard deviation of the energy spectrum.

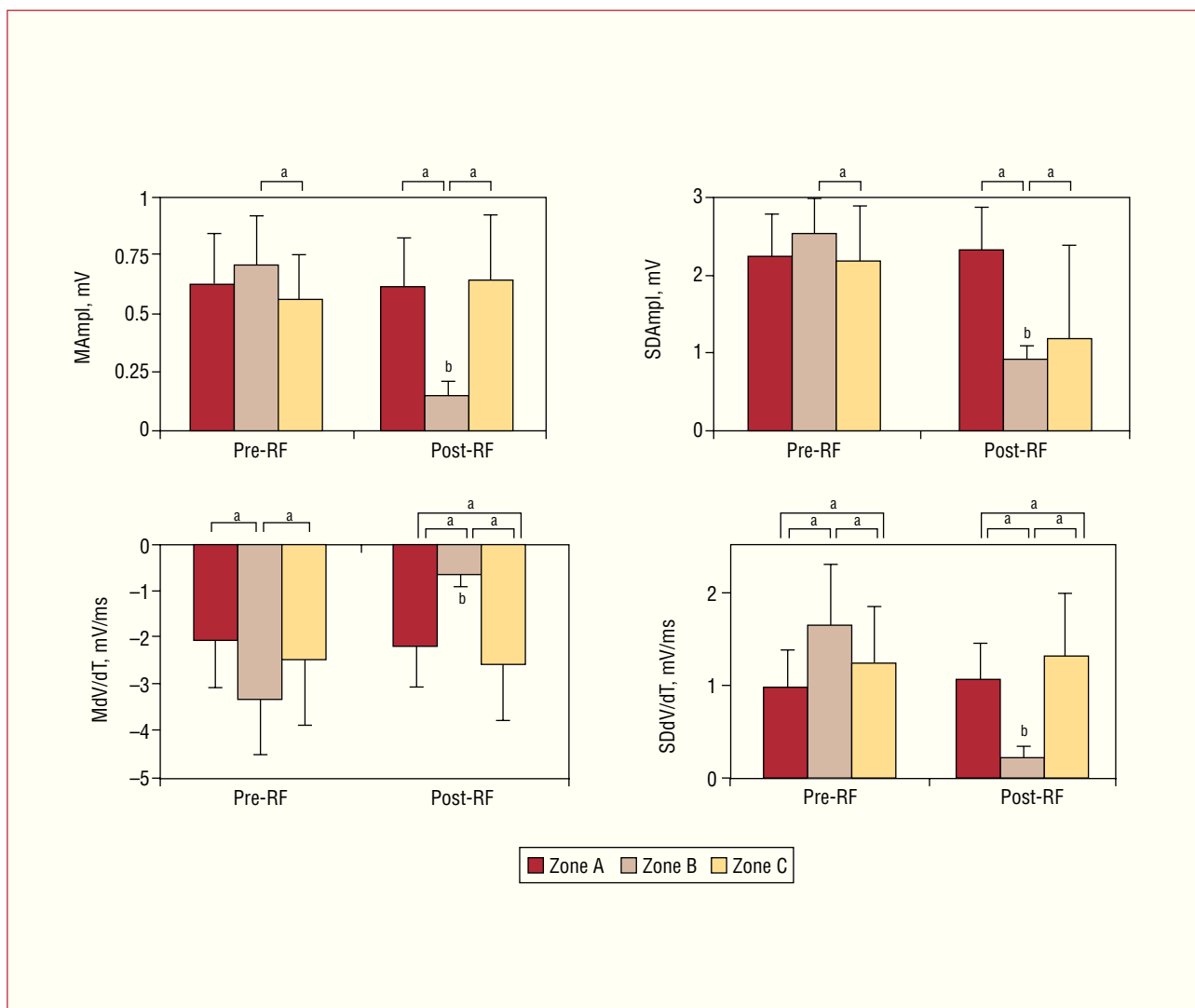


**Figure 5.** Values (mean [standard deviation]) of time domain parameters which varied significantly in the damaged zones. MAmpl, mean signal amplitude; MdV/dt, mean of the maximum negative slope of all electrograms; RF, radio-frequency; SDAmpl indicates standard deviation of signal amplitude; SDdV/dt, standard deviation of the electrogram's maximum negative slope; <sup>a</sup>Significant differences between zones: baseline and post-RF ablation. <sup>b</sup>Significant differences with respect to baseline values.

in adjacent, undamaged myocardium.<sup>9-11,23,25,27-29</sup> The analysis of the electrograms generated in the atrial or ventricular zones with RF lesions, both during sinus rhythm and in the context of certain arrhythmias, showed variations in the amplitude and speed of the deflections, with a reduction in the maximum negative slope.<sup>7-9,11-13</sup> Alterations in repolarization with changes in the amplitude of the T wave and displacements in the ST segment were also observed.<sup>29</sup> The decrease in amplitude has been used as a marker of a lesion in ventricular myocardium,<sup>12,13</sup> although the amplitude can decrease as a result of a deficient contact with the electrodes.<sup>30</sup> Chronic myocardial ischemia reduces the voltage of ventricular electrograms,<sup>31</sup> and the recording of distant signals can also reduce this

**TABLE 2. Odds Ratios and 95% Confidence Intervals for Parameters Accepted for Incorporation in the Logistic Regression**

	OR	95% CI
Frequency domain		
SDEsp, mV <sup>2</sup> /Hz	0.021	0.0067-0.0700
densMFr, mV <sup>2</sup> /Hz	0.3227	0.1278-0.8149
Time domain		
MdV/dt, mV/ms	0.0044	0.0002-0.0814
SDAmpl, mV	0.0118	0.0005-0.3015

CI, confidence interval; densMFr, spectral density of the mean frequency; MdV/dt, mean dV/dt; OR, odds ratio; SDAmpl indicates standard deviation of the signal amplitude in the ventricular fibrillation; SDEsp, standard deviation of the energy spectrum.

parameter's usefulness.<sup>13,32</sup> On the other hand, zones of post-infarct scarring give rise to similar changes as those produced by RF and it has been observed that electrogram voltage is correlated with the presence of ventricular scars.<sup>33,34</sup> The decrease in the density of viable myocytes in the infarcted regions leads to a reduction in electrogram amplitude and a reduction in the speed of the unipolar signals.<sup>35</sup> Experience gained in mapping studies has shown that information obtained by analyzing amplitude, the negative slope of the electrograms, or the duration of the signals can help in identifying scarred tissue.<sup>3,4,33,36</sup> Alternative methods to evaluate RF lesions have also been studied, including the increase in the stimulation threshold after ablation.<sup>13</sup> In the present study, the analysis of VF recordings confirmed that the lesions caused by RF can also significantly alter VF parameters in the time domain and that the indicators obtained are useful in differentiating between damaged and undamaged myocardium.

### **Modification of VF Frequency Domain Characteristics in Zones With lesions**

Spectral analysis of VF has been used to obtain information on myocardial activation during arrhythmia and the modifications produced by several factors including drugs, ischemia, stretching, or variations in temperature.<sup>14-17</sup> Because it alters the electrophysiological properties of the myocardium and the characteristics of the electrograms, RF ablation also modifies their spectral characteristics.

The dominant frequency corresponds to the frequency with the greatest spectral density and is closely related to the inverse of the mean activation cycles during VF. When we analyzed parameters directly related with the activation frequency, such as DFr or MFr, we found that they were not useful in distinguishing normal myocardium from damaged myocardium. These findings are related to the recording of distant potentials originating with the depolarization of the undamaged myocardium surrounding the lesions. However, as mentioned above, the potentials recorded in zones with lesions showed a considerable decrease in amplitude secondary to tissue coagulation necrosis and the loss of potentials generated during local depolarization.<sup>13,32</sup> Thus, while DFr and MFr, did not vary significantly in the damaged zone, the parameters related with the power and spectral energy varied significantly and were found to be useful in distinguishing between damaged and undamaged myocardium. The area under the ROC curve and the sensitivity, and specificity obtained separately for each parameter are similar to those obtained for the parameters in the time domain. The OR and their 95% CI obtained in the logistic regression analysis indicate the utility of these parameters in

identifying zones with lesions, in a similar fashion to those in the time domain.

The practical consequences of applying this type of analysis during VF will be determined from the results of experimental studies designed to further knowledge of the effects of RF ablation in ventricular arrhythmias. Bearing in mind that spectral analysis of atrial fibrillation has been used to identify regions of interest<sup>20,21</sup> and that these zones can be the target for therapeutic interventions, the study of the different parameters provided by this type of analysis could allow for a more rational use of RF ablation by broadening our knowledge of the phenomena involved. Using extracellular electrograms to identify zones with lesions helps to broaden our understanding of the characteristics of myocardial activation during electrical stimulation or arrhythmias. The present study has focused on the analysis of modifications in the signals recorded during VF and, while the analysis of the signals produced during atrial fibrillation is increasingly frequent in electrophysiological studies and during RF ablation procedures, signal recording during VF is less so. This is due to a large degree to the clinical characteristics of the arrhythmia itself. Nevertheless, this type of analysis provides additional information on the substrate and can help us to better understand this type of arrhythmia at a pathophysiological level.

### **Limitations**

The results were obtained in an experimental model using epicardial recordings. This allowed for precise control both when causing the RF lesions and when placing the recording electrodes. However, the sensitivity and specificity cut-points are dependent on the model and the animal species used. For that reason, extrapolating these results to a clinical setting requires additional, specific studies. The results presented were also analyzed in the acute phase after production of the RF lesions. The scarring process, whilst it would not modify the loss of capacity to generate potentials in the necrotized zone, could alter the passive transmission of potentials generated in the undamaged zones. Further studies using chronic models are required to analyze any changes and their consequences.

### **CONCLUSIONS**

During ventricular fibrillation, the spectral parameters associated with spectral power and spectral energy were significantly altered in zones with radiofrequency lesions and could be used to identify those zones. There was no significant change in either the dominant or mean frequency in these zones.



## REFERENCES

1. Stevenson WG, Friedman PL, Kocovic D, Sager PT, Saxon LA, Pavri B. Radiofrequency catheter ablation of ventricular tachycardia after myocardial infarction. *Circulation*. 1998;98:308-14.
2. Soejima K, Suzuki M, Maisel WH, Brunckhorst CB, Delacretaz E, Blier L, et al. Catheter ablation in patients with multiple and unstable ventricular tachycardias after myocardial infarction: Short ablation lines guided by reentry circuit isthmuses and sinus rhythm mapping. *Circulation*. 2001;104:664-9.
3. Zeppenfeld K, Kies P, Wijffels MC, Bootsma M, van Erven L, Schalij MJ. Identification of successful catheter ablation sites in patients with ventricular tachycardia based on electrogram characteristics during sinus rhythm. *Heart Rhythm*. 2005;2:940-50.
4. Verma A, Marrouche NF, Schweikert RA, Saliba W, Wazni O, Cummings J, et al. Relationship between successful ablation sites and the scar border zone defined by substrate mapping for ventricular tachycardia post-myocardial infarction. *J Cardiovasc Electrophysiol*. 2005;16:465-71.
5. Brunckhorst CB, Delacretaz E, Soejima K, Jackman WM, Nakagawa H, Kuck KH, et al. Ventricular mapping during atrial and right ventricular pacing relation of electrogram parameters to ventricular tachycardia reentry circuits after myocardial infarction. *J Intervent Cardiac Electrophysiol*. 2004;11:183-91.
6. Marchlinski FE, Callans DJ, Gottlieb CD, Zado E. Linear ablation lesions for control of unmappable ventricular tachycardia in patients with ischemic and nonischemic cardiomyopathy. *Circulation*. 2000;101:1288-96.
7. Schwartzman D, Kuck KH. Anatomy-guided linear atrial lesions for radiofrequency catheter ablation of atrial fibrillation. *Pacing Clin Electrophysiol*. 1998;21:1959-78.
8. Schumacher B, Jung W, Lewalter T, Wolpert C, Lüderitz B. Verification of linear lesions using a noncontact multielectrode array catheter versus conventional contact mapping techniques. *J Cardiovasc Electrophysiol*. 1999;10:791-8.
9. Taylor GW, Walcott GP, Hall JA, Bishop S, Kay GN, Ideker RE. High-resolution mapping and histologic examination of long radiofrequency lesions in canine atria. *J Cardiovasc Electrophysiol*. 1999;10:1467-77.
10. Chorro FJ, Mainar L, Sanchis J, Cánoves J, Llavador E, Such LM, et al. Mapping of atrial activation patterns after inducing contiguous radiofrequency lesions: An experimental study. *Pacing Clin Electrophysiol*. 2001;24:147-56.
11. Chorro FJ, Mainar L, Cánoves J, Sanchis J, Such LM, Porres JC, et al. Características de los electrogramas auriculares registrados en las líneas de bloqueo producidas con radiofrecuencia en un modelo experimental. *Rev Esp Cardiol*. 2000;53:1596-606.
12. Azegami K, Satake S, Okishige K, Sasano T, Ohira H, Yamashita K. Monitoring the local electrogram at the ablation site during radiofrequency application for common atrial flutter. *Jpn Circ J*. 1998;62:559-64.
13. Delacretaz E, Soejima K, Brunckhorst CB, Maisel WH, Friedman PL, Stevenson WG. Assessment of radiofrequency ablation effect from unipolar pacing threshold. *Pacing Clin Electrophysiol*. 2003;26:1993-6.
14. Chorro FJ, Guerrero J, Cánoves J, Martínez-Sober M, Mainar L, Sanchis J, et al. Quantification of the modifications in the dominant frequency of ventricular fibrillation under conditions of ischemia and reperfusion: an experimental study. *Pacing Clin Electrophysiol*. 1998;21:1716-23.
15. Chorro FJ, Cánoves J, Guerrero J, Mainar L, Sanchis J, Such L, et al. Alteration of ventricular fibrillation by flecainide, verapamil and sotalol. An experimental study. *Circulation*. 2000;101:1606-15.
16. Chorro FJ, Guerrero J, Ferrero A, Tormos A, Mainar L, Millet J, et al. Effects of acute reduction of temperature on ventricular fibrillation activation patterns. *Am J Physiol Heart Circ Physiol*. 2002;283:H2331-40.
17. Chorro FJ, Trapero I, Guerrero J, Such LM, Cánoves J, Mainar L, et al. Modification of ventricular fibrillation activation patterns induced by local stretching. *J Cardiovasc Electrophysiol*. 2005;16:1087-96.
18. Chorro FJ, Guerrero J, Trapero I, Such-Miquel L, Mainar L, Cánoves J, et al. Análisis tiempo-frecuencia de la fibrilación ventricular. Estudio experimental. *Rev Esp Cardiol*. 2006;59:869-78.
19. Chorro FJ, Guerrero J, Pelechano F, Trapero I, Mainar L, Cánoves J, et al. Influencia del tipo de registro (unipolar o bipolar) en las características espectrales de los registros epicárdicos de la fibrilación ventricular. Estudio experimental. *Rev Esp Cardiol*. 2007;60:1059-69.
20. Ryu K, Shroff SC, Sahadevan J, Martovitz NL, Khrestian CM, Stambler BS. Mapping of atrial activation during sustained atrial fibrillation in dogs with rapid ventricular pacing induced heart failure: Evidence for a role of driver regions. *J Cardiovasc Electrophysiol*. 2005;16:1348-58.
21. Lin YJ, Tai CT, Kao T, Tso HW, Higa S, Tsao HM, et al. Frequency analysis in different types of paroxysmal atrial fibrillation. *J Am Coll Cardiol*. 2006;47:1408-9.
22. Oppenheim A, Schaffer R. Digital signal processing. Englewood Cliffs: Prentice Hall; 1975.
23. Huang SK, Bharati S, Lev M, Marcus FI. Electrophysiologic and histologic observations of chronic atrioventricular block induced by closed-chest catheter desiccation with radiofrequency energy. *Pacing Clinical Electrophysiol*. 1987;10:805-16.
24. Lopez Merino V, Chorro FJ, Sanchis J, García Civera R, Such L, Camaño A, et al. Induction of complete AV block in dogs by transcatheter ablation using high-frequency current: An alternative to direct current high energy shock. *Eur Heart J*. 1989;10:113-9.
25. Wu CC, Fasciano RW, Calkins H, Tung L. Sequential changes in action potential of rabbit epicardium during and following radiofrequency ablation. *J Cardiovasc Electrophysiol*. 1999;10:1252-61.
26. Franz MR, Sharkey H, Edwards S, Scheinman MM. Real-time monitoring of radiofrequency-induced myocardial lesions by simultaneous recording of monophasic action potentials. En: Franz MR, editor. Monophasic action potentials: bridging cell and bedside. Armonk: Futura; 2000. p. 807-21.
27. Haines DE, Watson DD. Tissue heating during radiofrequency catheter ablation: A thermodynamic model and observations in isolated perfused and superfused canine right ventricular free wall. *Pacing Clin Electrophysiol*. 1989;12:962-76.
28. Nath S, Haines DE. Biophysics and pathology of catheter energy delivery systems. *Prog Cardiovasc Dis*. 1995;37:185-204.
29. Cinca J, Tapias A, Carreño A, Warren M, Mont L, Blanch P, et al. Local repolarization abnormalities induced by transcatheter radiofrequency ablation in pigs. *Pacing Clin Electrophysiol*. 1997;20:1952-60.
30. Reddy VY, Wroblewski D, Houghtaling C, Josephson ME, Ruskin JN. Combined epicardial and endocardial electroanatomic mapping in a porcine model of healed myocardial infarction. *Circulation*. 2003;107:3236-42.
31. Fuchs S, Kornowski R. Correlation between endocardial voltage mapping and myocardial perfusion: implications for the assessment of myocardial ischemia. *Coronary Artery Disease*. 2005;16:163-7.
32. Harada T, Stevenson WG, Kocovic DZ, Friedman PL. Catheter ablation of ventricular tachycardia after myocardial infarction: Relation of endocardial sinus rhythm late potentials to the reentry circuit. *J Am Coll Cardiol*. 1997;30:1015-23.
33. Thiagalingam A, Wallace EM, Campbell CR, Boyd AC, Eipper VE, Bit K, et al. Value of noncontact mapping for identifying left ventricular scar in an ovine model. *Circulation*. 2004;110:3175-80.
34. Keck A, Hertting K, Schwartz Y, Kitzing R, Weber M, Leisner B, et al. Electromechanical mapping for determination of myocardial contractility and viability: a comparison with echocardiography, myocardial single-photon emission computed tomography, and positron emission tomography. *J Am Coll Cardiol*. 2002;40:1067-74.

35. Wolf T, Gepstein L, Dror U, Hayam G, Shofti R, Zaretzky A, et al. Detailed endocardial mapping accurately predicts the transmural extent of myocardial infarction. *J Am Coll Cardiol.* 2001;37:1590-7.
36. Wroblewski D, Houghtaling C, Josephson ME, Ruskin JN, Reddy VY. Use of electrogram characteristics during sinus rhythm to delineate the endocardial scar in a porcine model of healed myocardial infarction. *J Cardiovasc Electrophysiol.* 2003;14:524-9.